Introduction

Pioneered by Tarantola (1984), full waveform inversion (FWI) is a powerful method that forms estimates of subsurface properties by iteratively minimizing a measure of the discrepancy between observed and modelled data. Multiparameter versions of FWI seek estimates of multiple physical subsurface properties (Virieux and Operto, 2009). Elastic full waveform inversion is a multiparameter formulation seeking estimates of the three independent elastic parameters required to characterize an isotropic elastic medium, commonly p-wave velocity, s-wave velocity, and density. While formulations for elastic FWI have existed for decades (Tarantola, 1986), their successful application to land data has been hampered by the computational overhead and nonlinearity involved in multiparameter inversion. While FWI for land applications has been explored Brossier et al. (2009), its success is limited to very small problems and numerical studies generally consider frequencies not normally recorded in the field.

Recent advances in sensor technology have created a novel means of acquiring seismic data known as distributed acoustic sensing (DAS). Employing optical fibres, DAS senses the strain due to seismic waves along the tangential component of the fibre. Interesting opportunities arise from the inclusion of DAS data in FWI. Encouragingly, DAS fibres are non-invasive, allowing them to be placed in producing wells, monitoring wells, and treatment wells. This property of DAS allows for greater access to data at transmission angles, increasing the information provide about long wavelength characteristics of the model, and further reducing cycle skipping. Additionally, distributed acoustic sensing has a well-documented ability to provide the very low frequency information (Jin and Roy, 2017; Becker and Coleman, 2019), that holds potential to mitigate cycle skipping.

Geophones and distributed acoustic sensors offer an opportunity to record datasets that are complementary both in the geometries they afford, and in the portion of the wavefield they sample. Geophones are challenging to deploy downhole, especially in horizontal wells where either a dedicated horizontal or well shut-in would be required. Distributed acoustic sensors offer a solution by allowing sensors to be deployed in producing wells without the need for dedicated monitoring wells, offering greater access to downhole acquisition. Conversely geophones are better suited to surface acquisition than DAS fibre. Access to these complementary datasets has the potential to improve inversion results. Full waveform inversion has typically considered geophone data and there is little previous work in using DAS, or a combination of DAS and geophone data. Here we present a method for FWI of DAS data from shaped fibres that is flexible in its ability to incorporate data from arbitrarily shaped and oriented fibre. The method presented here can also simultaneously invert geophone and DAS data, leveraging the complementary aspects of each dataset.

Theory

Conventionally, full waveform inversion minimizes the discrepancies in modelled data $\mathbf{Ru}$ and observed data $\mathbf{d}$, by considering a problem of the form,

$$\min_{\mathbf{m}} \frac{1}{2}||\mathbf{Ru}-\mathbf{d}||_2^2 \qquad \text{subject to} \qquad \mathbf{Su}=\mathbf{f}. \tag{1}$$

Equation (1) is an optimization problem constrained by the requirement that the wave equation is satisfied, where S is a wave equation operator, in this paper the operator for the isotropic elastic wave equation, and $\mathbf{f}$ is the source function. The matrix $\mathbf{R}$ handles properties of the receivers in computing the modelled data from the modelled wavefield. In the case of geophones it performs the function of sampling the displacement wavefield at the locations of the receivers.

The optimization problem in equation (1) is often solved using gradient-based methods and provides an estimate of the subsurface parameters $\mathbf{m}$ that is consistent with the observed data. These require gradient calculations, which can be computed using the method of Lagrange multipliers and the adjoint state method (Metivier et al., 2013). The gradient being given by,

$$\frac{\partial \phi}{\partial \mathbf{m}} = \left\langle \frac{\partial \mathrm{S}}{\partial \mathbf{m}} \mathbf{u}, \lambda \right\rangle \tag{2}$$

which is the cross-correlation of the forward modelled wavefield $\mathbf{u}$ and an adjoint wavefield λ. The adjoint wavefield can be computed through the solution to the adjoint wave equation

$$\mathrm{S}^{\dagger}\lambda = \mathbf{R}^{\mathrm{T}}(\mathbf{R}\mathbf{u} - \mathbf{d}). \tag{3}$$

The preceding objective function and gradient are typically employed to invert data recorded by geophones. However, it is important to note that in the objective function no assumption was made about the form of the receiver matrix $\mathbf{R}$. Additionally, the gradient is computed through partial derivatives of the objective function with respect to the model parameters. Because the receiver matrix is independent of the model parameters, it may be altered without affecting the form of the gradient in equation (2). This allows $\mathbf{R}$ to handle any properties of the receivers we desire while retaining the same expressions for the objective function and gradient used in FWI with geophone data. Through careful construction of the receiver matrix, the expressions in equations (1), (2), and (3) can be used to invert the data supplied DAS fibres.

Inversion of DAS data

The fibres used in distributed acoustic sensing are sensitive to the portion of the wavefield causing strain along the tangential direction of the fibre. The data supplied by DAS is thus inherently different than the data supplied by geophones, and careful formulation of the receiver matrix is required for its inclusion in FWI. The response of a DAS fibre to a strain field can be computed through the projection of the strain field onto a coordinate system that contains the fibre tangent. For 2D wavefield simulations the expression for the response of a DAS fibre in terms of the Cartesian strain field $(\varepsilon_{xx}, \varepsilon_{xz}, \varepsilon_{zz})$ is given by Innanen (2017) as,

$$\varepsilon_{\mathrm{tt}} = (\hat{\mathbf{t}} \cdot \hat{\mathbf{1}})^2 \varepsilon_{xx} + 2(\hat{\mathbf{t}} \cdot \hat{\mathbf{1}})(\hat{\mathbf{t}} \cdot \hat{\mathbf{3}})\varepsilon_{xz} + (\hat{\mathbf{t}} \cdot \hat{\mathbf{3}})^2 \varepsilon_{zz}. \tag{4}$$

where $\hat{\mathbf{t}}$ is a unit vector in the direction of the fibre tangent, and $\hat{\mathbf{1}}$ and $\hat{\mathbf{3}}$ are Cartesian unit vectors.

Equation (4) shows the response of the DAS fibre is a weighted sum of the Cartesian strain components, where the weights are a function of the tangential direction of the fibre and are therefore dependent on the geometry of the fibre. Wrapping the fibre in geometric shapes, such as a helix, alters the tangent direction, reducing the redundancy of the supplied measurements. In practice the fibre response at a point along the fibre is the spatial average of the tangential strain over a distance along the fibre centered on that point. This distance is known as the gauge length and with current technology is on the order of 10 meters. In this paper we invoke the gauge length by averaging the fibre sensitivities over one finite difference cell, giving one fibre strain measurement per cell that contains a fibre segment.

The receiver matrix in FWI of geophone data samples the modelled wavefield at the locations of the geophones in forming the modelled data. To extend FWI to the data supplied by DAS receivers we formulate $\mathbf{R}$ to incorporate the properties of DAS receivers, resulting in an objective function whose minimization reduces discrepancies in observed and modelled DAS strain data. Specifically, $\mathbf{R}$ is formulated to compute the strain field from the displacement field, which is achieved through a finite difference approximation to the expression for the strain tensor. This strain field is then projected onto the coordinate system of the fibre using the weights in equation (4) and the expression of the rotation for a rank 2 tensor (e.g. Krebes (2019)). Gauge length averaging is then invoked by computing the average of these weights within the finite difference cell. These three functions of $\mathbf{R}$ supply the modelled DAS strain response within a finite difference cell consistent with equation (4).

Examples

To compare inversions from geophone data, and those from simultaneous inversions of geophone and DAS data we investigate a numerical example. A portion of the elastic Marmousi model is used as the true model, with an acquisition geometry that considers surface sources. The starting model for ρ, v_p and v_s are linear gradients. Two inversions for different receiver geometries are considered, one with surface geophones, and one with surface geophones supplemented by buried fibre.

The left panel of figure 1 shows a segment of the fibre used to acquire the DAS strain data used for FWI. This fibre is constructed from periodic segments of fibre consisting of 4.5 winds of a helical fibre with a wind angle of 19.25 degree connected by a half wind of helical fibre wound at 59.5 degrees. The right panel of figure 1 shows the sensitivity of this fibre to the ε_{xx} (top right), ε_{xz} (middle right), and ε_{zz} (bottom right) both point-wise (blue) and averaged over the gauge length (green). Importantly a fibre of this type has significant sensitivity to all three strain components in the 2D case.

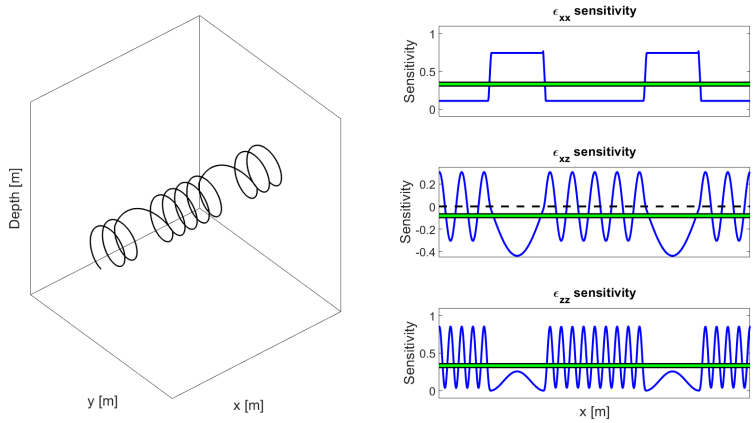

Figure 1 *Section of fibre used for DAS sensing of the strain data used in FWI (left). Sensitivity of this fibre to each component of strain for ε_{xx} (top right), epsilon$_{xz}$ (middle right), and ε_{zz} (bottom right). The blue lines show the point-wise sensitivity of this fibre, while the green line represents the gauge length averaged strain.*

Figure 2 shows the inversion result from surface geophones (row 2), and a simultaneous inversion of surface geophone and buried DAS fibre (row 3). Because our formulation uses the same objective function and gradient for both geophone and DAS data, both can be simultaneously included in the inversion by using an appropriate expression for **R**. The inversion considers only frequencies above 10 Hz, simulating what may be expected from conventional 3C geophones. With a lack of low frequency information, the inversion that considers only surface geophone data struggles to properly characterize the long wavelength aspects of the model, especially deeper in the model, as shown in the second row of figure 2. The inclusion of data from a buried DAS fibre in the inversion provides access to long wavelength information from transmission data. The inversion benefits from the inclusion of this type of data as shown in the third tow of figure 2. The long wavelength characteristics of the inverted models, especially for v_p and v_s are a better match to the true models when considering geophone and DAS data compared to geophone data alone.

Conclusions

Distributed acoustic sensing is growing in popularity as a technology for seismic acquisition, especially in downhole applications. With their growing application, it is important to develop strategies for the inclusion of the data they provide in parameter estimation, in order to leverage the supplemental information they afford. Access to these complementary datasets has the ability to improve inversion results as shown by the example in figure 2. Here we develop a method for the inversion of DAS data from

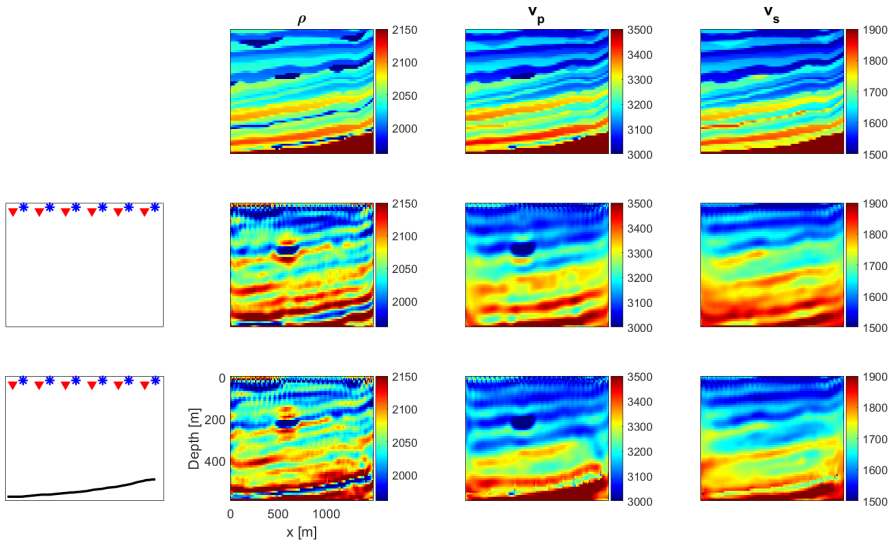

Figure 2 *Inversion results from a portion of the elastic Marmousi model for* ρ *(second column),* v_p *(third column),* v_s *(fourth column). The top row shows the true model used to generate the observed data, the second row the inversion result from inverting data from surface geophones and the third row the inversion result from simultaneous consideration of data from surface geophones and buried DAS fibre. The left column provides a schematic representation of the acquisition geometries for each geometry with sources shown by the blue stars, geophone by the red triangles, and DAS fibre by the black line.*

arbitrarily complex fibre geometries, that allows for the simultaneous inversion of DAS and geophone data. The simultaneous inclusion of both datasets in FWI provides access to complementary geometries and portions of the wavefield that improve parameter estimates over considering either dataset alone. Future work will investigate structuring **R** to be frequency dependent, placing a greater emphasis on DAS data at very low frequencies and incorporating geophone data as the bandwidth increases.

Acknowledgements

The authors would like to thank the sponsors of the CREWES project as well NSERC under the grant CRDPJ 461179-13 for making this work possible through their financial support. Matt Eaid and Scott Keating were partially supported through scholarships from the SEG Foundation.

References

Becker, M. and Coleman, T. [2019] Distributed acoustic sensing of strain at Earth tide frequencies. *Sensors*, **19**(9), 1975.

Brossier, R., Operto, S. and Virieux, J. [2009] Seismic Imaging of complex onshore structures by 2D elastic frequency-domain full-waveform inversion. *Geophysics*, **74**(6).

Innanen, K.A. [2017] Parameterization of a helical DAS fibre wound about an arbitrarily curved cable axis. *79th EAGE Conference and Exhibition*.

Jin, G. and Roy, B. [2017] Hydraulic-fracture geometry characterization using low-freqeuncy DAS signal. *The Leading Edge*, **36**(12), 962–1044.

Krebes, S. [2019] *Seismic Wave Theory*. Cambridge University Press, 1 edn.

Metivier, L., Brossier, R., Virieux, J. and Operto, S. [2013] Full waveform inversion and the truncated newton method. *Siam J. Sci. Comput.*, **35**, B401–B437.

Tarantola, A. [1984] Inversion of seismic reflection data in the acoustic approximation. *Geophysics*, **49**(8), 1259–1266.

Tarantola, A. [1986] A strategy for nonlinear elastic inversion of seismic reflection data. *Geophysics*, **51**, 1893–1903.

Virieux, J. and Operto, S. [2009] An overview of full-waveform inversion in exploration geophysics. *Geophysics*, **74**(6), WCC127–WCC152.